Tuning Barrier Properties of Biological Hydrogels

Jennifer L. Schiller[a], Samuel K. Lai[a,b,c]*

[a]Division of Pharmacoengineering and Molecular Pharmaceutics, Eshelman School of Pharmacy; [b]UNC/NCSU Joint Department of Biomedical Engineering; [c]Department of Microbiology & Immunology; University of North Carolina at Chapel Hill, Chapel Hill, NC 27599

*Corresponding author:
Samuel K. Lai
Eshelman School of Pharmacy
Division of Pharmacoengineering and Molecular Pharmaceutics
University of North Carolina at Chapel Hill
Marsico 4213, 125 Mason Farm Road
E-mail: lai@unc.edu
Homepage: http://www.lailab.com

Target journals: ACS Applied Bio Materials
Title: 6 words

Abstract (words: 173)

A major function of biological hydrogels (biogels) is to serve as barriers against invading pathogens and foreign materials. This review focuses on methods to tune the steric and adhesive barrier properties of biogels at the nanoscale. Altering the biogel mesh spacings that lead to changes in steric obstruction allows for gross exclusion of larger particles, but does not provide selectivity with molecular specificity. Enabling direct binding of specific entities to the biogel microstructure introduces specificity, yet has very limited breadth, unable to block numerous diverse entities. In contrast, third party modulators that interact with the biogel matrix to enable crosslinking of specific entities to the biogel mesh, and/or facilitate agglutination of these entities, can robustly tune the barrier properties of biogels against multiple species with molecular specificity without direct chemical modification of the biogel or changes to its microstructure. We review here the design requirements for developing effective third party modulators. The ability to selectively enhance the barrier properties of biogels has important implications for numerous applications, including prevention of infection and contraception.

1 Introduction

Hydrogels are three-dimensional networks of polymers that are able to swell and retain large quantities of water. We define biological hydrogels (biogels) as hydrogels comprised of biologically derived polymers, ranging from simple polysaccharides (e.g. agarose) to complex glycoproteins (e.g. mucins), held together by entanglements and/or adhesive bonds between the major structural biopolymers. These bonds can be either reversible or irreversible, including disulfide bonds, hydrogen bonds (H-bonds), as well as ionic and hydrophobic forces that can be influenced by factors such as ions, pH, and temperature.[1] For example, alginate can reversibly gel in the presence of calcium and other divalent cations.[2] Collagen I is soluble in weakly acidic solutions, but gels upon neutralization and heating via a combination of inter-residue electrostatic and hydrophobic interactions.[3] Agarose, upon supersaturation at a temperature above its gelation point, will gel upon cooling due to H-bonding between ester and alcohol groups.[4] Silk fibroin hydrogels can be fabricated by passing an electric current through solution and ionizing the water, forming locally acidic areas.[5]

Formation of irreversible, covalent chemical crosslinks may also occur directly between matrix constituents or via addition of exogenous crosslinkers. For instance, Schiff reactions between aldehydes from homobifunctional crosslinkers and amines on a polymer of interest has been used to induce gelation in both silk fibroin[5] and chitosan.[6] Carbodiimide catalyzes esterification of alginate chains, thus forming a gel.[7] Hyaluronic acid (HA) grafted with dextran-tyramine conjugate can be enzymatically crosslinked via tyramine groups with horseradish peroxidase.[8] These

reversible/irreversible adhesive crosslinks, coupled with physical polymer entanglements, are responsible for the macro-rheological (i.e. mechanical) properties of the biogels, and prevent otherwise soluble biogel polymers from simply dissolving in aqueous solution.

Biogels are ubiquitous in living systems. Biogels provide structural support for tissues and mechanical signaling for cells and are crucial for complex physiological processes such as passage of food along the GI tract, movement of joints, and reproduction. Biogels are also increasingly used for a variety of biomedical applications, including scaffolds for tissue replacement in severe burns and drug delivery systems that slowly release encapsulated therapeutics. While frequently overlooked, biogels also function as a selective barrier at the nano- to micro- scale that are essential for many physiological processes. Mucus, for example, lines the gut, female reproductive tract, and respiratory tract, excluding bacteria, viruses, and potential toxins from assessing the underlying epithelium while allowing for free exchange of essential nutrients and immune molecules.[9-12] Bacterial colonies form a similar protective coating in the form of a biofilm, a complex extracellular matrix composed of polysaccharides, proteins, DNA, and lipids that exclude antibiotics and immune system components, thus increasing the colony's chances of survival.[13-15] Basement membrane, a biogel composed primarily of collagen IV and laminin, likewise protects blood vessels and internal organs from pathogenic invasion.[16] It is this selective barrier function of biogels that we focus this review.

The penetration of proteins, viruses, motile bacteria, and nanoparticles through biogels can be hindered in two ways: (1) steric hindrance and (2) adhesive interactions. With steric obstruction, the spacings between structural elements of the gel must be sufficiently small relative to the foreign entities to physically exclude those entities based solely on their dimensions, with more effective exclusion when the size of the entity exceeds the dimensions of the mesh spacing. Entities can also directly bind to the structural elements of the gel, either through specific or non-specific adhesive interactions. Adhesive barrier properties of biogels are particularly important against entities that are too small to be slowed by steric obstruction and entities that possess active motility apparatuses that can displace the microstructure locally to create larger pores (e.g. sperm or bacteria with active motility) (Figure 1). In this review, we will discuss the biochemical and structural properties of biogels that enable their selective barrier functions, specifically emphasizing recent work on modifying biogel barriers through engineered third-party crosslinkers. Third-party crosslinkers flexibly and specifically extend the principles of steric hindrance and adhesive interactions. These crosslinkers can adhesively crosslink entities to biogel matrix via strong affinity to the foreign entity and weak affinity with the matrix. Other third-party crosslinkers may induce formation of aggregates, increasing the effective particle size and decreasing the flux of foreign species that can permeate through the biogel pores.

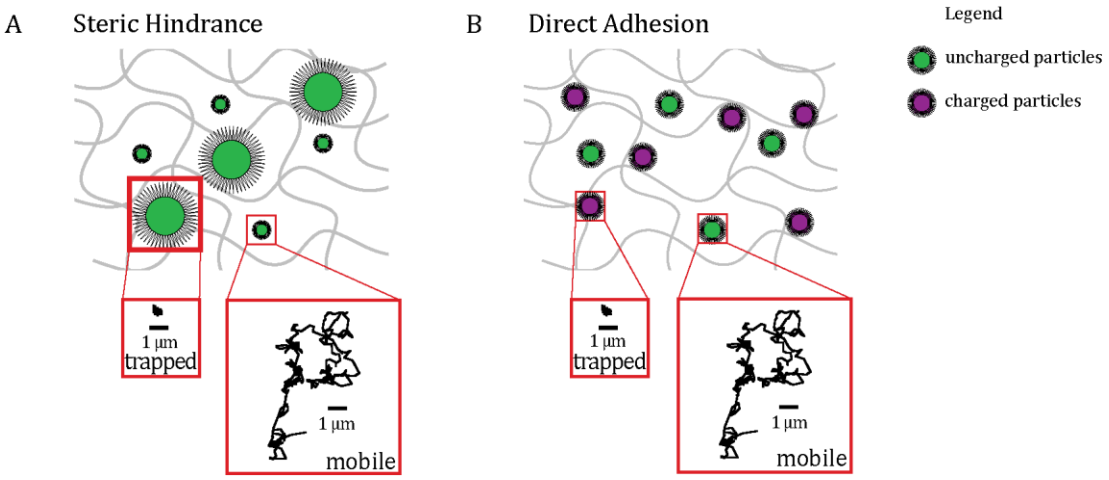

Figure 1. Barrier properties of hydrogels. **(A)** Diffusive green particles smaller than the mesh spacings are compared to larger green particles whose diameter approaches that of the matrix pore size, and thus are slowed by steric hindrance, as indicated by exemplary particle traces that span much smaller distances than the more diffusive traces of smaller nanoparticles. **(B)** Charged particles that are smaller than the mesh spacings can be trapped in the biogel matrix constituents via direct adhesion in contrast to similar sized but otherwise uncharged nanoparticles, resulting in marked difference in their permeability through the biogel(see Section 2.2. for details). Figure is original.

2 Steric and adhesive barrier properties of biogels

2.1 Characteristics of steric obstruction

Hydrogels, by definition, have characteristic pore sizes that vary based on polymer concentration, polymer chemistry, ionic strength, fiber thickness, and crosslinker density. In a purely viscous fluid, smaller particles diffuse faster than larger ones, with their mobility inversely correlated to their diameter; particles twice as large will diffuse twice as slowly. In a biogel of given mesh size, this difference can be particularly accentuated when the size of the larger particles is near or larger than the pores present, even if both particles do not adhesively interact with the biogel matrix. This is exemplified in human endotracheal mucus, in

which the diffusivities of 200 and 500 nm muco-inert nanoparticles were slowed to a much greater extent relative to their theoretical diffusivities in water than smaller 100 nm particles; the measured mean-squared displacements of 200 and 500 nm particles were 5- and 100-fold smaller than that of 100 nm particles at the same time scale, despite only a 2- and 5-fold difference in diameter, respectively.[17] Similar patterns are found in porcine respiratory mucus,[18] human cervicovaginal mucus,[19,20] mouse brain,[21] breast tumor cell interstitium,[22] and basement membrane.[23]

Biogels with smaller pores inherently exert greater steric obstruction than biogels with larger pores. It is then implicit that accurate assessment of the true steric barrier properties of a biogel are dependent on accurate assessment of the pore sizes present in the biogel. Unfortunately, pore sizes reported in the literature can vary widely depending on method of measurement (Table 1), which can be broadly classified into either static or dynamic methods. Static methods involve obtaining static images of the biogels, using scanning electron microscopy (SEM), transmission electron microscopy (TEM), atomic force microscopy (AFM), or confocal microscopy (of fluorescently labeled polymers). In contrast, dynamic methods estimate the pore sizes of biogels based on some form of diffusivity measures, such as fluorescent recovery after photo bleaching (FRAP), fluorescent correlation spectroscopy (FCS), multiple particle tracking (MPT), or swelling. Static methods appear to more often yield larger pore size estimates than dynamic methods in the literature. Erikson *et al.*[24] reported a side-by-side comparison with collagen I: using FRAP, they measured pore diameters that ranged from ~100 nm (20 mg/mL collagen) to ~500 nm (2 mg/mL collagen), whereas with confocal

reflection microscopy, pore sizes in the same collagen gels appeared to be at least three-fold larger, ranging from ~500 nm (20 mg/mL collagen) to ~1.2 μm (2 mg/mL collagen). Comparisons of hydrogel measurements between papers from the same research groups also reveal similar patterns. For example, SEM estimated 10 μm pores in a 35 mg/mL alginate $CaCl_2$ gel,[25] but a later paper measured pores of just 7-17 nm in alginate gels of 30-70 mg/mL using a size exclusion chromatography (SEC)-based method.[26]

The reason for the discrepancy in pore sizes measured between static vs. dynamic methods is not well-understood. Ramanujuan *et al.*[27] hypothesized that unassembled polymers between pores visible by microscopic techniques may increase the viscosity experienced by diffusing particles in the interstitial volume space, thus altering the calculated pore size. Erikson *et al.*[24] suggest the discrepancy is due to the failure of two-dimensional microscopic techniques to fully characterize the three-dimensional nature of hydrogels. Pore sizes measured can also be influenced by the methods for preparing gels for static imaging. To process hyaluronic hydrogels for SEM, Yang, *et al.*[28] freeze-dried and fractured gels, potentially introducing ice-crystals that artificially increases measured pore size, as suggested by the ~100-fold increase in pore size compared to dynamic measurement by Lin, *et al.*[29] This is further complicated by the difference in crosslinking techniques, as the former used BDDE with a drying step to crosslink, while the latter used photocrosslinking. In contrast, Lorén, *et al.*,[30], used glutaraldehyde, a crosslinker and fixative, and dehydration to prepare κ-carrageenan gels for TEM. These modifications may reduce changes to the pore size,

as reflected by the relatively small (~5-fold) increase compared to the similarly-prepared κ-carrageenan gels measured dynamically by NMR diffusometry by de Kort, *et al*.[31] These differences in preparation for pore size measurement do not, however, full explain the differences measured by static vs. dynamic strategies: the aforementioned Erikson *et al.*[24] study did not require additional preparation steps when measuring pore sizes by confocal reflection microscopy (static) or by FRAP (dynamic), yet calculated a 3-fold greater pore size by static method. Finally, it is possible that the entities measured using dynamic methods may actually be

Biogel	Measurement Method	Conc. (mg/mL)	Pore Size (diam.)	Prep. Method	Refs
Agarose	Dynamic	20	124 - 206 nm	Supersaturated and cooled	[32]
Alginate	Dynamic	30 - 70	7 - 17 nm	Added dropwise into 0.1M $CaCl_2$	[26]
	Static	35	10 μm	Added dropwise into 0.1M $CaCl_2$	[25]
Chitosan	Dynamic	10	3.5 nm	Water-swollen membrane	[33]
	Static	10 - 50	25 -240 μm	Water-swollen membrane	[34]
Collagen I	Dynamic	2 - 20	100 - 500 nm	Incubated at 37°C	[24]
	Static	2 - 20	300 nm - 1.2 μm	Incubated at 37°C	[24]
Hyaluronic acid	Dynamic	20	300 - 500 nm	Photocrosslinked	[29]
	Static	20	50 - 100 μm	Crosslinked with 0.4-1% BDDE at 40°C, then dried and reswelled	[28]
κ-carrageenan	Dynamic	10 - 50	5 - 7 nm (lower limit)	Incubated with 200 mM NaCl and 20 mM KCl	[31]
	Static	2.5 - 30	25 - 95 nm	Incubated with 200 mM NaCl and 20 mM KCl	[30]

Table 1. Pore sizes of select biogels. BDDE- 1,4-butanediol diglycidyl ether.

interacting at least weakly and transiently with the matrix, therefore slowing those entities more than would be predicted from steric obstruction alone. Ultimately, we recommend dynamic measurements when possible to determine functional pore size.

2.2 Adhesive barrier properties

To overcome steric obstruction, many species in nature either have evolved to be substantially smaller than the mesh pore sizes, employ active diffusion, and/or possess the ability to deform themselves. Motile bacteria and eukaryotic cells can overcome the steric obstruction for a biogel by effectively squeezing through smaller pores and/or directing motion with flagella or pseudopodia. However, when examining the diffusion of nanoparticles in complex biogels, a general pattern emerges: charged (both positive and negative) particles, even those markedly smaller than the mesh spacings in the biogels, are often immobilized, whereas neutral particles diffuse freely. Hindered mobility or complete immobilization of charged particles is consistently observed in basement membrane,[23,35-38] human cervicovaginal mucus (CVM),[19,39] human respiratory mucus,[17] breast tumor parenchema,[23] vitreous humor,[40,41] and purified porcine gastric mucins.[42] In contrast, particles with a near-neutral zeta potential, often through grafting polyethylene glycol (PEG) to the particles, exhibit much more rapid diffusion in the same biogels despite similar hydrodynamic diameters to the charged particles. This

has been demonstrated in CVM,[19,43-45] human airway mucus,[17] basement membrane,[23] breast tumors,[23] F-actin,[46] and fibronectin[46] (summarized in Table 2).

Biogel	Net Charge	Type of Particles Trapped	Refs
F-actin	Negative	Negative	46
Fibronectin	Negative	Negative	46
Basement membrane	Negative	Negative, positive	35,38
Alginate	Negative	Negative	47
Mucus			
Airway	Negative	Negative, positive	17,48,49
Cervicovaginal	Negative	Negative, positive	19,39,44,50,51
Gastrointestinal	Negative	Negative, positive	52

Table 2. Adhesive interactions in select biogels.

Arends *et al.*[35] probed the mechanism of these adhesive interactions by measuring the rate of positively charged, negatively charged, and neutral nanoparticles in basement membrane. In a concentration-dependent manner, salts in excess of physiological salt concentration increased the mobility of charged particles that were otherwise immobile in basement membrane. The same group later reported similar findings in the vitreous humor.[40] Excess salts act to shield the charges on the nanoparticles and/or the hydrogels, preventing these charges from interacting with each other, suggesting an electrostatic mechanism. The specific character of these charge-charge interactions, whether ionic or charge-assisted H-bonding, was not determined.

Attractive electrostatic forces trap more strongly than repulsive forces. In a model of mixed positively and negatively charged dextrans, Hansing *et al.*[53] measured the mobility of fluorescent molecular probes with net negative charges. As the ratio of positively charged dextran to total dextran decreased, the effective

diffusivity of the molecular probe increased, suggesting the negatively charged fluorescent probes were interacting primarily with the positively charged dextran. To clarify the relative strength of attractive vs. repulsive interactions, Griffiths *et al.*[54] investigated the interactions of porcine gastric mucins with nanoparticles. Mucins are densely decorated with sialic acid and, as such, have a strong net negative charge. When incubated with mucins, positively charged nanoparticles, but not negatively or neutrally charged nanoparticles, exhibited a marked increase in their hydrodynamic diameter as measured by dynamic light scattering, indicating that the attractive electrostatic forces can drive surface adsorption of mucus. Not surprisingly, nanoparticles coated with positively charged electrolytes displayed a marked reduction in their effective diffusivity in gastrointestinal porcine mucus compared to those with near neutral coatings of a similar diameter.[52]

Interestingly, repulsive electrostatic forces can also adversely impact particle mobility in biogels. Stylianopoulos *et al*.[55] explored the effect of repulsive electrostatic interactions and found that in a generic negatively charged gel at physiologic ionic strength, repulsive forces were relevant for diffusing particles only around very small particles, i.e. those with diameters near the Debye length. This effect is more pronounced in solutions of lower ionic strength or with a higher fiber volume fraction. Unsurprisingly, increased particle surface charge density from 0 to 0.1 C/m^2 decreased diffusivity, of a magnitude related to ionic strength and fiber volume fraction.

Less intuitively, strongly charged nanoparticles can also be trapped in similarly charged biogels. For example, densely carboxylated polystyrene beads, which are negatively charged, are immobile in neutralized CVM, which carries a strong net negative charge.[39,50,56,57] In this instance, carboxylic acid on the beads and sialic acids on mucins can form strong H-bonds with each other, sharing an environmental proton, due to the stabilizing forces of their respective negative charges, resonance, and similar pKa values.[58] The sheer number of H-bonds due to the density of carboxylic acid groups on both beads and mucins can create high avidity crosslinks that effectively immobilize negatively charged beads.

Hydrophobic particles are also trapped in biological hydrogels with hydrophobic domains through hydrophobic interactions. This is perhaps best studied in the context of oral drug absorption in the gastric mucosa. Larhed *et al.*[59,60] has extensively studied the diffusivity of drugs ranging in lipophilicity from logK -3.5 to logK 3.3 using a mucus-coated diffusion chamber. They found a negative correlation between lipophilicity and diffusivity in porcine intestinal mucus, hypothesized to be due to interactions with the hydrophobic naked protein domains on mucins. Similarly, Groo *et al*.[61] used a Transwell chamber to demonstrate that free paclitaxel, a notoriously hydrophobic molecule, diffuses far more slowly through porcine intestinal mucus than in a hydrophilic, PEGylated lipid nanocarrier form, although the latter has a much larger hydrodynamic radius. Together, these studies indicate a role for hydrophobic interactions with the biogel matrix can also impede permeability through biogels.

Finally, the native adhesive barrier properties can vary substantially due to environmental factors such as pH. For instance, HSV[20,45] and HIV VLPs[50,62] are immobile in native CVM, which has a pH of 3.5-4.0 due to lactic acid secreted from commensal *Lactobacillus* bacteria, but can readily diffuse through pH-neutralized CVM (mimicking the pH-buffering effects of alkaline semen) with mean squared displacement about 1000 times greater than that at pH 4. Trapping is likely due to H-bonding between sugars on mucins and sugars on glycoproteins of HIV, as more of both are protonated at a lower pH and thus can more easily form H-bonds.

3 Tuning the barrier properties of biogels

3.1 Altering steric obstruction of biogels through changing its microstructure

It follows that to impede the diffusion of particles by steric hindrance, one must decrease the pore size of the hydrogel (Fig. 2). This can be done by increasing the crosslinking density of polymers, altering pore size mechanically through methods of forming hydrogels, and increasing the concentration of the polymer. As discussed above, biogels require some combination of entanglement and/or crosslinking to form an insoluble gel. Increasing the density of crosslinkers or using more potent crosslinkers will increase the frequency of crosslinks within the gel, thus decreasing the effective pore size.

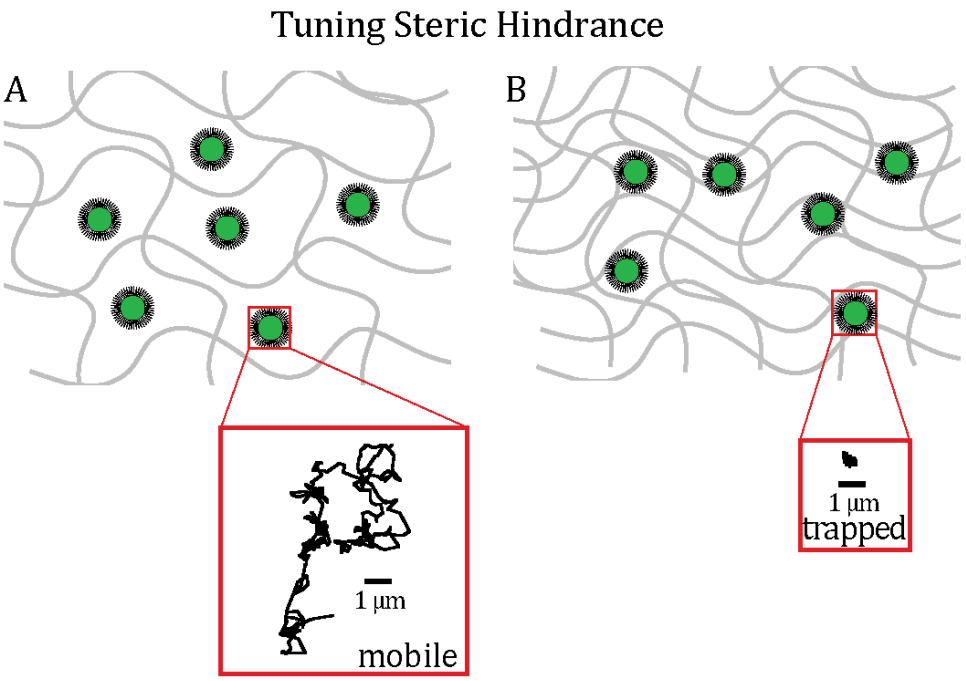

Figure 2. Tuning steric hindrance of biogels. **(A)** Particles that do not associate with the matrix constituent and consequently mobile in the biogel will become immobilized when **(B)** the pore size of the biogel is decreased to smaller than the size of the particles. Figure is original.

3.1.1 Tuning crosslinking of biogels

Arends *et al.*[36] examined the mobility of particles within reconstituted murine basement membrane from the Engelbroth-Holm-Swarth sarcoma (dry mass 60% laminin, 30% collagen IV) from several sources. Corning's Matrigel®, the source with the highest concentration of the laminin crosslinker entactin, reduced the diffusive fraction of 200 nm PEG nanoparticles to 0%, compared to 70-80% in samples with the lowest concentration of entactin. Increased crosslinker density was correlated with a 4-fold stiffer gel, markedly smaller pore sizes, and, not surprisingly, reduced nanoparticle mobility (Figure 3). Conversely, particles and cells can gain greater mobility when crosslinking density is reduced, such as via photolytic degradation of the crosslinkers. Kloxin *et al.*[63] encapsulated cells in PEG

diacrylate with a photodegradable crosslinker based on nitrobenzyl ether, followed by masked flood irradiation to spatially erode a channel. Cells in or near the channel were released and became migratory along the proscribed path due to the resultant increase in pore size. Chemical degradation of crosslinks, exemplified by reduction of disulfide bonds by N-acetylcysteine in airway mucus from patients with cystic fibrosis, has a similar effect: the fraction of mobile 200 nm and 500 nm PEG-coated nanoparticles increase by ~2- and ~6-fold, respectively.[64] Schultz and Anseth[65] found a correlation between crosslink density and rheological properties in an enzymatic model of crosslink degradation, using MPT to probe the microrheological properties of peptide-crosslinked PEG-norbornene hydrogels. As the ratio of matrix metalloproteinase-degradable crosslinkers to nondegradable crosslinkers was increased, collagenase treatment had a correspondingly greater effect on the diffusivity of microparticle probes. Hydrogels with a nondegradable/degradable crosslinker ratio above a critical threshold demonstrated no change in probe diffusivity upon degradation by collagenase.

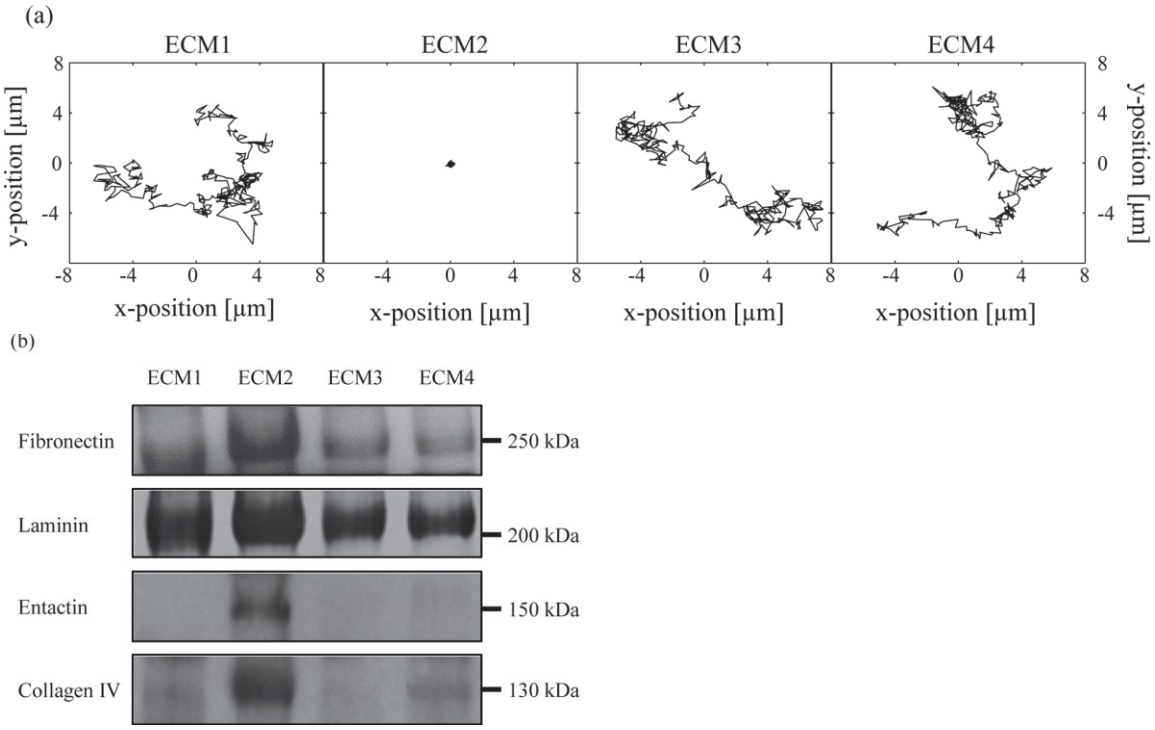

Figure 3. Particle mobility and content of ECM proteins in foure different ECM gel variants. (a) Exemplary trajectories of PEGylated particles with a diameter of 200 nm in the four different gels. Trajectories are shifted for clarity. (b) The content of fibronectin, laminin, entactin and collagen type IV in the four different ECM gels is analyzed by western blot. Figure adapted from [36].

The density of crosslinks can also differ based on the crosslinking efficiency of the crosslinkers themselves. For example, the pore sizes of HA gels, composed of polymeric disaccharides of glucuronic acid and N-acetyl glucosamine, can vary by ~30% simply by changing the crosslinker from divinely sulfone to ethylene glycol diglycidyl ether.[66] Likewise, chitosan, consisting of deacetylated chitin, exhibits a 2-fold smaller mesh size, 8-fold greater crosslink density, and 6-fold stiffer gel when ionotropically gelled with tripolyphosphate instead of pyrophosphate, demonstrating a correlation between mesh size, crosslink density, and bulk

rheology.[67] Further methods to crosslink hydrogels have been reviewed by Ullah *et al*.[68] and Akhtar *et al.*[69]

3.1.2 Methods to form hydrogels

Porosity of gels can be tuned through methods of forming hydrogels such as salt leaching, porogens, gas foaming, electrospinning, and freeze-drying. These methods have been extensively reviewed elsewhere.[70,71] Briefly, salt leaching, porogens, and gas foaming all induce porosity by causing gelation to occur around a solute or gas bubble, which is then removed by evaporation or immersing the gel in a specific solvent. The sizes of salt crystals, porogens, and bubbles directly influence the pore sizes. For example, Kim *et al.*[72] used NaCl crystals in the formation of silk fibroin scaffolds, followed by leaching of the crystals from the scaffolds, and found the resultant pore size to be within 10% of crystal size. Freeze-drying involves rapidly freezing a biogel and removing solvent, which also leaves behind pores. The temperature at which this occurs affects the final pore size. In another preparation of silk fibroin scaffolds, Mandal *et al.*[73] found that lower freezing temperatures are correlated with smaller pore sizes, with a two-fold difference between gels frozen at -20°C and those frozen at -196°C. Electrospinning is the only additive method; it creates polymeric fibers of defined size that collectively become a porous scaffold. Huang *et al.*[74] varied polymer concentration, flow rate, liquid nitrogen, needle thickness, and temperature of collector to vary both fiber and pore diameter of electrospun silk fibrinogen over a six-fold range. Further techniques have been extensively reviewed by Vedadghavami *et al*.[75] and Bajaj *et al.*[76]

3.1.3 Tuning polymer concentration

Intuitively, greater amounts of polymer present in a biogel will increase entanglements and effective crosslinks between polymer strands, and consequently, increase steric obstruction of particles in the biogel (unless the increased polymer concentration only results in thicker or more bundled fibers). Indeed, increasing the concentration of F-actin by ~10-fold slowed the diffusion of 1.04 μm polystyrene microspheres by ~10-fold.[77] Similarly, in a collagen I model, an increase in polymer concentration from 2 mg/mL to 20 mg/mL the diffusion of 2MDa dextran by 3-fold.[24]

Not surprisingly, selective reduction of polymer, such as by enzymatic degradation, increases the effective mesh spacings and decreases steric hindrance of particles in biogels. The vitreous humor of the eye is composed of a network of fibrous collagen and HA, crosslinked by proteoglycans. Treatment with collagenase, trypsin, and hyaluronidase all increased the pore size and nanoparticle diffusivity within the eye, with the greatest effect achieved with collagenase, implicating the outsized structural role of fibrous collagen compared to HA in the vitreous gel. Magzoub *et al.*[78] examined the diffusion of dextrans with FRAP in tumor ECMs before and after digestion of collagen I, decorin, or HA. While digestion of collagen I and decorin each increased dextran diffusivity, digestion of HA actually decreased dextran diffusivity.

3.1.4 Stimuli-responsive steric tuning

Many of these aforementioned techniques are static in nature, requiring the perturbation to be part of the creation of the biogel. This has led a number of investigators to develop so-called "smart" hydrogels that can directly respond to changes in their environment. These have gained popularity in recent decades in the drug delivery field, with the aim of using these gels to increase compliance and fine-tune dosing. An example application is in diabetes management, which seeks to create a closed-loop glucose-gated insulin delivery device- an implanted hydrogel that doses insulin depending on the available glucose in the blood. A longstanding challenge for insulin-dependent diabetics is insulin dosing and timing. Insulin needs vary, depending on carbohydrate consumption, health, hormones, activity level, and pancreatic function. Thus, even the most fastidious diabetic may have difficulty controlling their blood glucose levels during times of extreme stress or physical illness. Li *et al.*[79] immobilized glucose oxidase, glucose catalase, and insulin within pH-sensitive peptide hydrogels, testing for efficacy in diabetic mice (Figure 4). Increase in blood glucose levels led to metabolism of glucose by immobilized oxidase and catalase, resulting in a local decrease in pH, causing the hydrogel to swell. Upon swelling, the pores of the hydrogel increased and allowed for diffusion of insulin out of the gel. Released insulin decreased glucose levels, and the pH within the gel returned to physiological, shrinking the pores and retaining the remaining insulin. Many other smart approaches to glucose-responsive delivery, including from synthetic hydrogels and supramolecular assemblies of insulin derivatives, have

been expertly reviewed by Webber and Anderson[80] and VandenBerg and Webber.[81]

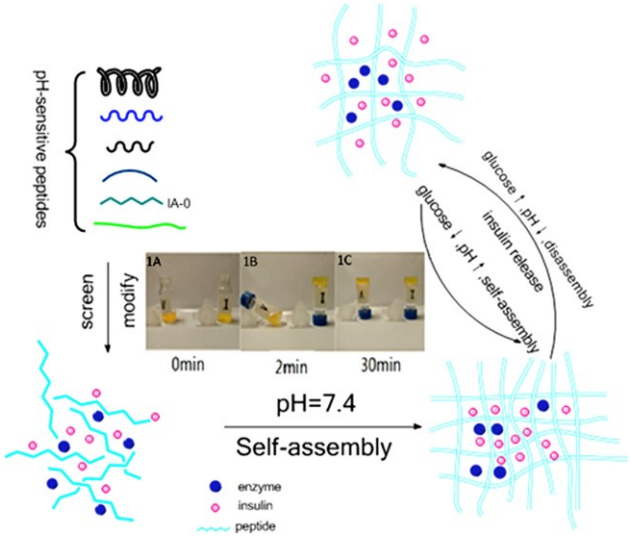

Figure 4. Diagram of the glucose-mediated insulin delivery system using pH-sensitive self-assembling peptide hydrogels. A, B and C indicate the process of the hydrogels formation. Figure from [79].

3.2 Direct adhesion to the biogel matrix

Electrostatic interactions are present in many naturally occurring hydrogels. Nevertheless, creating synthetic gels that can support electrostatic-based adhesion can be challenging. As many gels form through physical interactions that rely on the same functional groups that mediate electrostatic interactions, altering electrostatic properties may affect the rheological properties of the gel.

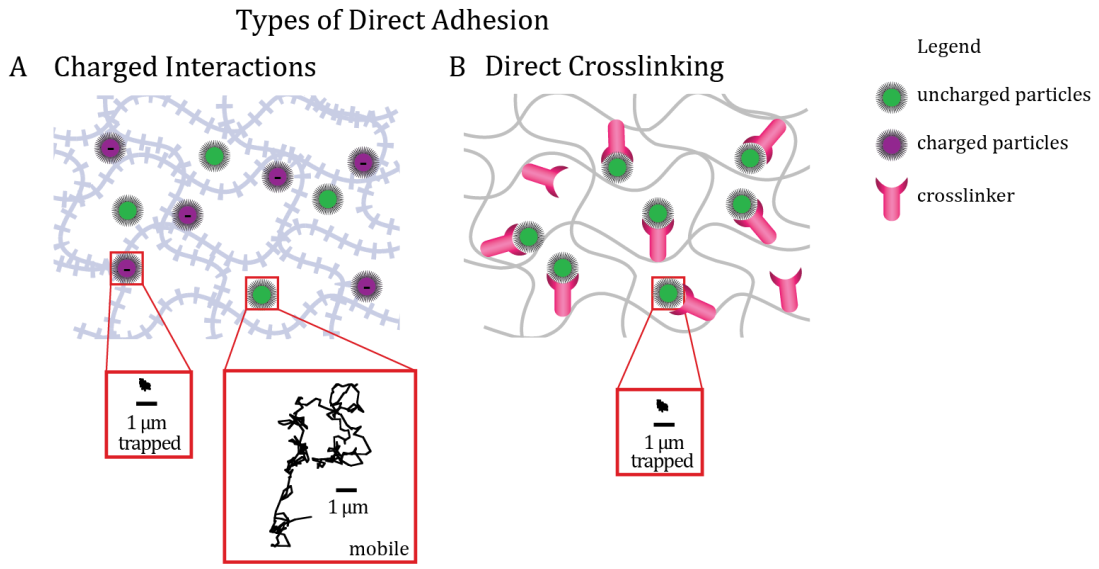

Figure 5. Types of direct adhesion. **(A)** Charged (purple) particles adhere directly to charged matrix constituents via charge-charge interactions, while uncharged (green) particles undergo rapid diffusion in the interstitial fluid space within the biogel. **(B)** Uncharged, mobile particles are trapped by crosslinkers that bind both nanoparticle and matrix components. Figure is original.

Adhesion by electrostatic interactions is also highly non-specific. Instead of non-specific electrostatic interactions, it is possible to tune the adhesive barrier properties of biogels with molecular specificity to direct modifications of the biogel matrix with ligands. This allows a discrete number of entities of interest to be trapped, while other entities of similar size and with similar electrostatic properties might remain mobile (Fig. 5).

One approach to overcome this problem is to modify a so-called "template" gel, onto which functional groups of interest can be conjugated onto an independently assembling hydrogel. Such strategies have been recently reviewed by Acar *et al.*,[82] Chen *et al.*,[83] and Liu and Hudalla.[84] These gels have the added benefit of allowing, but not requiring, target specificity. A particularly elegant solution is the

EAK16 peptides, which consist of 12-16 alternately charged (half positive and half negative) and hydrophobic residues that spontaneously self-assemble into β-sheet fibrillizing hydrogels with the hydrophobic residues in the interior. To tune charge specificity via electrostatic interactions, Gelain *et al.*[85] used three derivations of the RADA16 peptide to modify the surface of the formed protein scaffolds and measured the diffusion of positively and negatively charged cytokines in each of the gels. In the negatively charged RADA16-DGE gel, positively charged cytokines diffused at a quarter of the rate of negatively charged cytokines. In the positively charged RADA16-PFS gel, the negatively charged cytokines diffused at a tenth to a fifth of the rate of positively charged cytokines.

Freudenberg *et al.*[86] tackled the problem of charge-tuning hydrogels by using a non-biological hydrogel, star-shaped PEG, as a base gel to which different quantities of heparin and variously sulfated glycosaminoglycans could be conjugated, tuning both the number of ionizable sulfate groups per hydrogel volume and the charge density on the glycosaminoglycan component. Both the stiffness and swelling degree varied less than two-fold. Basic cytokines bound to the hydrogels in direct correlation to the number of ionizable sulfate groups per hydrogel volume, regardless of level of sulfation. Both acidic cytokines with positively charged heparin-binding domains and neutral cytokines bound to gels in a manner first correlating with charge density and then the number of ionizable groups per volume, although cytokines with heparin-binding domains bound more strongly overall. Acidic cytokines with no heparin-binding domain did not bind to the highly

negatively charged gels. These results are consistent with previous studies of electrostatic-based trapping in hydrogels.

In a model of more specific adherence to the matrix, Bodenberger *et al.*[87] covalently incorporated lectin B from *Pseudomonas aeruginosa* into albumin-based hydrogels to trap bacteria. Lectin B successfully captured a carbapenem-resistant clinical isolate of *P. aeruginosa* with enough affinity that it could not be washed off with PBS, although it could be eluted by a sugar with higher affinity for the lectin. A similar strategy[88] involving the non-covalent incorporation of lectins into a supramolecular peptide-based hydrogel was used to analyze the glycosylation patterns of intact glycoproteins. Lectins and fluorescence-enabling quenchers were immobilized in specific regions on a chip; trapped glycans and glycoproteins were added later. Lectin binding was detected by fluorescence, as binding released the competitive fluorescent quencher. This hydrogel was used to detect the concentration of glucose from a solution and identify the glycans present on several complex glycoproteins.

Many groups incorporate adhesion peptide sequences into hydrogels, such as those derived from fibronectin (RGD(S)) and laminin (IKVAV).[89-93] These sequences allow for integrin binding and have been successfully used to encourage cellular migration and proliferation. As such, they do not enhance the barrier function of hydrogels and are beyond the scope of this review.

3.3 Advantages and disadvantages of tuning steric hindrance and direct adhesion properties of biogels

Steric hindrance is a facile method to tune biogels to grossly exclude particles based strictly on their hydrodynamic diameter. It is ubiquitous in the majority of biogels, as exemplified by the subdiffusive behaviors of proteins, viruses, and nanoparticles in various biogels vs. in buffer.[51,94] The total exclusion of larger particles, and slowing of smaller particles, while non-specific, is an important barrier feature, and can be tuned in response to external stimuli. In addition to the ligand-sensing example discussed above, change in pH,[95] application of light,[63,96] and enzymatic degradation[97] have all been used to alter the steric hindrance of a biogel, often to facilitate *in vivo* drug release.

As discussed above, relying on steric hindrance alone to tune barrier properties results in only size-specific rather than molecule-specific exclusion. Additionally, decreasing pore sizes to the extent needed for effective exclusion may result in excess stiffening of the biogel, which in turn may impact other biological functions such as mucus clearance or cell attachment. Branco de Cunha *et al.*[98] probed the effect of stiffness of an interpenetrating alginate/collagen I network on fibroblast development and protein expression in the course of developing a wound dressing. They found that increasing stiffness from 50 Pa to 1200 Pa by increasing calcium crosslinking of alginate both inhibited fibroblast spreading and upregulated expression of inflammatory cytokines. This indicates that, should a hydrogel be designed for barrier purposes at wound sites, steric hindrance as the sole barrier mechanism may afford limited utility.

To block the permeation of entities that cannot be effectively slowed by tuning the pore sizes, such as those smaller than the mesh spacing or which possess active motility apparatuses that can displace mesh elements, harnessing adhesion to the matrix constituents represents a promising strategy. These direct adhesions confer molecular specificity and are useful in contexts in which selective permeability is desired. For example, mucus must balance protection of the underlying epithelium from pathogens and toxins with allowing exchange of nutrients. To this end, a number of studies, reviewed by Wagner *et al.*,[12] have demonstrated the interaction of microbes with unique mucin glycans, specifically preventing the penetration of both viruses and bacteria to the underlying epithelium.

However, tuning biogels via direct adhesion requires modification of the chemistry of the biogel itself. This is an inherently low-throughput process, necessitating a separate polymer be created for each target entity to be immobilized. It also prevents modification of the barrier properties of a biogel post fabrication. A biogel's permeability to various entities cannot be tuned in response to novel entities, nor could extant biogels be modified without the introduction of additional polymer. For these reasons, we believe third party modulators may be a preferable method for tuning barrier properties of biogels.

4 Third party modulators

Two categories of third party modulators exist: matrix-binding crosslinkers and agglutinators (Table 3). Matrix-binding crosslinkers in hydrogels combine the general utility of electrostatic interactions with the specificity of conjugating ligands directly to biogels. These crosslinkers incorporate two binding elements, with the most potent crosslinkers comprising a domain with low-affinity bonds to the biogel matrix and a domain that form high affinity bonds with specific epitopes on foreign species. Such matrix-binding crosslinkers can be administered before or after gelation, do not affect the gel's bulk rheological properties, can be administered to a native biogel (such as mucus), and require no creation of a *de novo* gel. This strategy also enables multiple entities of interest to be specifically trapped at once through the use of a cocktail of crosslinkers (Fig. 6).

	Matrix-Binding Modulators	**Agglutinating Modulators**
Interactions with Biogel	Weak and transient	Not necessary
Interactions with Particles	Many crosslinkers accumulate on one particle	Many crosslinkers interact with many particles to induce aggregation
Mechanism for Reduced Mobility	Adhesion to biogel matrix	Steric obstruction by the biogel matrix; reduced diffusivity/mobility
Requirements	Requires rapid diffusion of crosslinkers for efficient pathogen encounters	Requires high local concentrations of foreign species; most effective against foreign species with active motility
Example Application	Enhancing the CVM barrier against sexually transmitted infections; facilitating rapid clearance of respiratory viruses from the lung	Limiting sperm permeation of cervical mucus for non-hormonal contraception; induction of enchained growth in the GI tract to maintain homeostatic bacterial populations
Refs	44,48,99-101	102-108

Table 3. Key properties of third-party modulators.

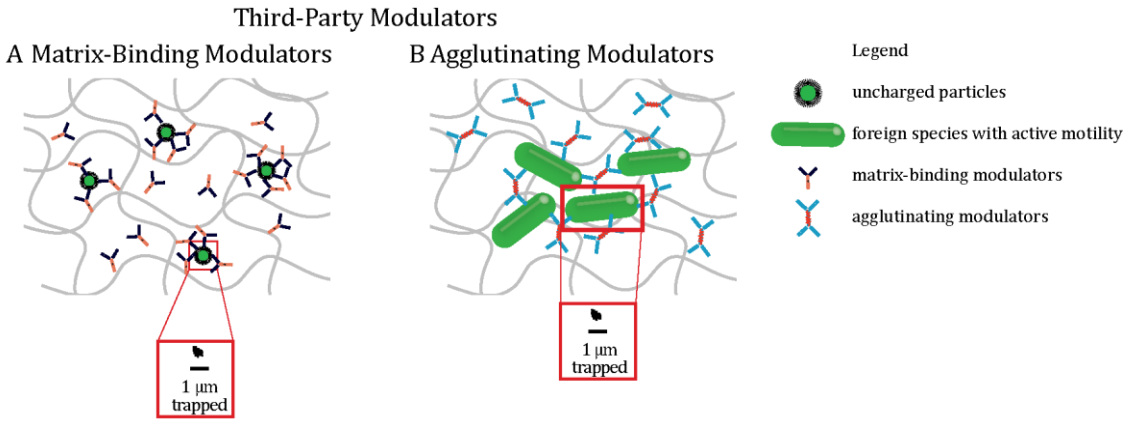

Figure 6. Types of third party modulators. A) Matrix-binding modulators immobilize particles through transient, weak interactions with matrix constituents. B) Agglutinating modulators crosslink multiple particles together in clumps too large to diffuse through the matrix, without needing to interact with the matrix directly. Figure is original.

Agglutinating crosslinkers function by agglutinating or enchaining particles into a mass too large to diffuse through matrix pores or to engage in active mechanisms to effectively mobilize. These agglutinating crosslinkers' potencies depend on their polyvalency; multivalent crosslinkers like IgA or IgM are far more potent at agglutination than bivalent IgG. The crosslinker need not interact with the matrix, allowing more flexibility in the biogel in which it can be used.

4.1 Third party crosslinking to biogel matrix

Our group has pioneered the use of IgG antibodies as matrix-binding crosslinkers in biological hydrogels to immobilize viruses, bacteria, and nanoparticles. Initially, we discovered that the mobility of herpes simplex virus (HSV) in CVM was inversely proportional to the endogenous level of anti-HSV IgG in the CVM specimen. We showed that addition of exogenous anti-HSV IgG into CVM with low endogenous anti-HSV IgG caused otherwise readily mobile HSV to become

completely immobilized. Non-neutralizing, anti-HSV IgG was able to effectively reduce vaginal Herpes transmission in mice, but protection was critically dependent on the presence of mucus.[44] We have since demonstrated that IgG-mediated trapping of HSV is consistent across the menstrual cycle and in women with diverse vaginal microbiota[109] and that IgG- and IgM-mediated trapping can limit access to the underlying epithelium.[39] IgGs that bind Ebola virus-like particles (VLPs) also effectively immobilized them in human airway mucus (AM) and facilitated rapid clearance of Ebola VLPs from the mouse airway.[48] High endogenous levels of anti-influenza antibodies are similarly correlated with low mobility of influenza VLPs in the human AM.[110] Exogenous addition of anti-LPS IgG to mouse gastrointestinal mucus (GIM) lacking endogenous antibodies reduced the fraction of actively motile *Salmonella typhimurium*, increasing their tendency to undergo hindered or diffusive motion rather than swim in a directed fashion.[102]

Antibody-mediated trapping is not exclusive to mucus gels. In basement membrane as well as biogels comprised of its principal structural component, laminin, IgG and IgM effectively immobilized nanoparticles to the matrix. They can also retard the migration of bacteria across the gel.[38] Similar IgG- and IgM-mediated immobilization of nanoparticles has been found in alginate.[47]

4.1.1 Physical mechanism of third party crosslinkers that adhesively crosslink to matrices

Previous work has shown that IgG possess only very weak affinity to mucins. This suggests matrix-binding IgG crosslinkers involve both highly specific, high-affinity interactions between the target entity and crosslinker and low-affinity

interactions between the crosslinker and the matrix constituents. This contrasts with the conventional paradigm that high-affinity matrix-crosslinker bonds should promote more potent trapping. To evaluate the role of matrix-crosslinker affinity on trapping potency, we anchored IgG to the matrix of basement membrane via biotin-avidin chemistries.[99] Instead of enhancing trapping potencies, we found that high-affinity bonds between the crosslinker and matrix actually strongly reduced trapping potency (Fig. 7). High affinity bonds with the matrix most likely limited the diffusional freedom of the crosslinker, which in turn compromised the ability of the crosslinker to quickly bind to the target entity of interest. This implies that in the presence of high crosslinker-matrix affinity, any successful bond between the crosslinker and target entity is limited by the diffusion of the target entity, which is typically much slower (e.g. HIV, with a diameter ~100nm, is ~20x larger than an IgG), leading to much slower k_{on} and thus lower trapping potencies.

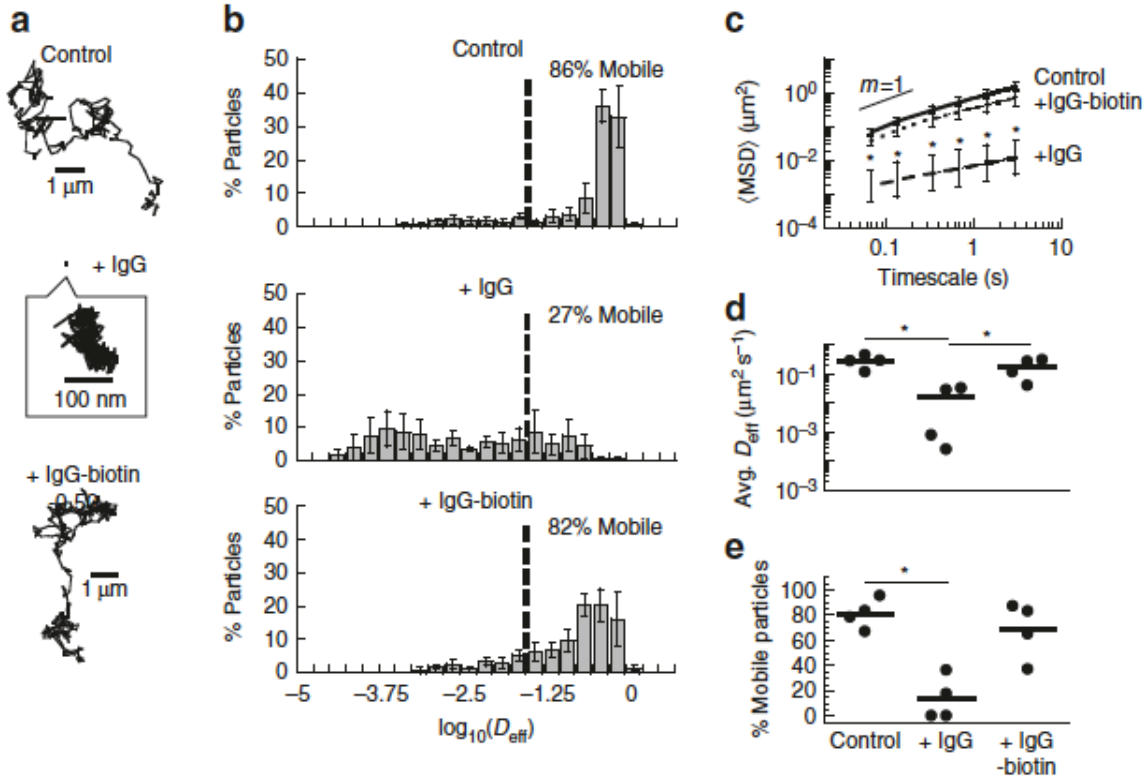

Figure 7. Transient vs. stable anchor-matrix bonds. Diffusion of 200 nm polyethylene glycol (PEG)-conjugated latex nanoparticles in biotinylated Matrigel® modified with neutravidin. (A) Representative traces of nanoparticles in Matrigel® with no added IgG (control), anti-PEG IgG (IgG), or biotinylated anti-PEG IgG (IgG-biotin) exhibiting effective diffusivities within one SEM of the ensemble average at a timescale of 1 s. (B) Distributions of the mean logarithms of individual particle effective diffusivities (D_{eff}) at a timescale of 0.2667 s. Log (D_{eff}) values to the left of the dashed line correspond to particles with displacements of less than 100 nm (i.e., roughly the particle diameter) within 0.2667 s. c Ensemble-averaged geometric mean square displacements (<MSD>) as a function of timescale, (D) mean Deff of all particles in each condition, and (E) fraction of mobile nanoparticles in Matrigel® treated with different IgG. N = 4 separately prepared slides/condition with 83–237 particles tracked per slide. Error bars represent SEM. *p < 0.05 compared to control in indicated comparisons. p values were calculated by repeated measures two-way ANOVA in (C), with one-way ANOVA on log-transformed data in (D), and with one-way ANOVA in (E). Reproduced with permission.[99]

In contrast, crosslinkers with weak matrix-crosslinker interactions can bind and unbind from the matrix constituent rapidly, allowing them to diffuse through the matrix and quickly encounter, bind, and accumulate on the target entities of

interest. When a sufficient number of crosslinkers accumulate on a pathogen, despite continued binding/unbinding events by individual crosslinkers, at least one pathogen-bound crosslinker will most likely remain bound to the matrix, thereby effectively trapping the pathogen-crosslinker complex.

In good agreement with our experimental observations, Monte Carlo simulations also confirmed that weak, transient bonds between the crosslinker and the matrix are critical to reinforcing the biogel barrier. In a computational model of HIV diffusing through CVM to reach epithelial cells, Chen *et al.*[101] showed that even slowing the diffusion of IgG by just 20% relative to in buffer (i.e. α=0.8), which reflects the affinity of IgG to midcycle cervical mucus,[94] was sufficient to reduce the quantity of HIV virions penetrating CVM and reaching the underlying epithelium by >90% over the course of two hours, compared to IgGs with no affinity to mucins. A later study by Wessler *et al.*[100] expanded on this paradigm and found that to limit HIV diffusion through mucus, the optimal crosslinker affinity to matrix is achieved when the diffusivity of the crosslinker is slowed by ~75% in matrix compared to in buffer, which is comparable to the affinity between IgM antibodies and mucins. With greater crosslinker-matrix affinity (i.e. >75% slowed in matrix than water), the ability to trap virus actually decreased. In addition to weak affinity to the matrix, rapid diffusivity of the crosslinker is also important to maximize the rate of crosslinker accumulation on the entity of interest. Newby, et al.[99] found that nanoparticles need to be far larger than crosslinkers: a 20x increase in size of the nanoparticle compared to crosslinker increases trapping efficiency ~4x. Moreover,

crosslinkers that form weak, transient bonds with the matrix more potently prevented the penetration of nanoparticles across the barrier than did crosslinkers that form long-lasting, strong bonds with the matrix by an order of magnitude.

4.1.2 Molecular mechanism of transient crosslinker-matrix interactions

As part of the initial discovery that anti-HSV IgG traps HSV in CVM, Wang *et al.*[44] identified the component on IgG that mediated the interactions with mucins. A $F(ab)_2$ construct, produced by removal of Fc by pepsin digest, completely abrogated trapping. Deglycosylation of the two conserved Fc glycosylation sites at Asn297 with PNGase F also similarly abrogated the trapping potencies of IgG (Fig. 6). This led to the conclusion that Fc glycans are integral to IgG-mediated trapping in cervicovaginal mucus.

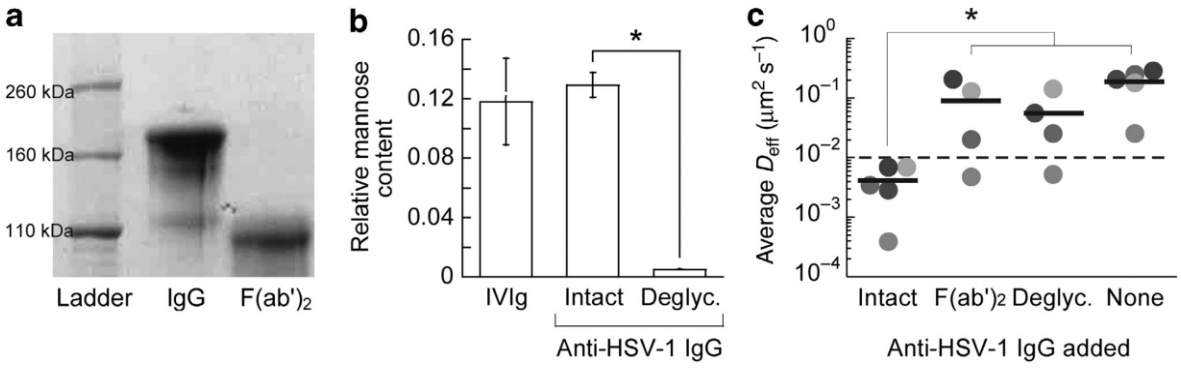

Figure 8. Deglycosylation of IgG abrogates trapping of HSV in CVM. (A) Fc removal from anti-HSV1, confirmed by SDS-PAGE. (B) Deglycosylation of anti-HSV1, confirmed by lectin-ELISA. (C) Effective diffusivity of HSV1 in the CVM treated with intact, Fc-removed, and deglycosylated IgG. Reproduced with permission.[44]

Motivated by studies with various mucus secretions, we explored whether IgG and IgM could also facilitate trapping in other biogels, and discovered that both mediated effective trapping of virus-sized nanoparticles in Matrigel® as well as matrix comprised of laminin/entactin.[38] Notably, IgM antibodies have 51 potential

glycosylation sites. Of these, 31 are glycosylated with complex glycans terminated in galactose or sialic acid and are 80% occupied. The remaining 20 are glycosylated with oligomannose and are 17% or 100% glycosylated, depending on location.[111] We deglycosylated IgG with PNGase F and IgM with a cocktail of endoglycosidases and found a reduction in trapping. Again, we concluded that glycans on antibodies are necessary for this crosslinking to occur.

The weak, transient, polyvalent immobilization induced by third party crosslinkers indicates H-bonding as the likely driving force behind this interaction. As deglycosylation of antibodies negates all trapping, we believe this H-bonding involves glycans. Hydroxyl, carboxylic acid, and N-acetyl groups on glycans are all capable, to varying ability, of participating in H- bonding. Charged groups, such as carboxylic acid at pH 7, produce stronger bonding, whereas neutral groups, such as hydroxyl, produce much weaker bonding. IgG glycans are often terminated in N-acetylglucosamine or galactose, but less frequently sialic acid. Their ability to mediate trapping in alginate, but not agarose, similarly to the differential ability of desialylated IgM to mediate trapping in alginate only, suggests that terminal galactose or small quantities of N-acetlyglyucosamine forms bonds insufficient to trap particles. Fully sialylated IgM, which possess 16-20 sialic acid groups/Ab, has an abundance of carboxylic acid and N-acetyl groups to participate in H- bonding. In alginate, carboxylic acid provided by the biogel can interact with the abundant remaining hydroxyl groups, compensating for the loss of carboxylic acid and N-acetyl groups on the IgM. Agarose provides only hydroxyl groups for interaction,

and hydroxyl-hydroxyl, or even hydroxyl-N-acetyl, H-bonds are not particularly strong compared to charge-assisted carboxylic acid-hydroxyl or carboxylic acid-carboxylate H-bonds.[112]

4.2 Harnessing agglutination to enhance steric obstruction with molecular specificity

Immune exclusion describes the ability for polyvalent antibodies such as sIgA and IgM to agglomerate many pathogens together. This creates a clump that is either too large to diffuse through mucus and/or is unable to swim in a coordinated fashion towards any particular direction. Antibody need not interact with the matrix to induce agglutinates. Agglomerated pathogen complexes, similar to pathogens that are crosslinked to mucins, are quickly eliminated by natural mucosal clearance mechanisms, such as ciliary beating in the respiratory mucosa or peristalsis in the intestinal mucosa.[113] Immune exclusion has long been proposed as the mechanism by which sIgA protects the mucosal epithelial from bacteria.[108]

4.2.1 Third-party modulators that induce agglutination

Sperm, self-propelled by vigorously beating flagella, must swim through mucus to fertilize the egg. In the 1970s and 1980s, Kremer and Jager discovered the "shaking sperm" phenomenon in infertile couples: sperm that appeared as large aggregates too large to passively diffuse through the pores of cervical mucus and unable to undergo any coordinated motion due to head-to-head configurations of spermatozoa but which shook in place as the sperm were otherwise active.[105] The shaking phenomenon was associated with high titers of anti-sperm IgG, sIgA, and/or IgM antibodies in either semen or mucus.[104-106,114] Indeed, agglutinating anti-sperm

antibodies administered to rabbit CVM effectively agglutinated sperm *in vivo* and reduced fertility to almost 0% in a dose-dependent manner.[115]

Agglutination is critically dependent on the concentration of the target entity, as these entities must be colliding with each other with sufficient frequencies in order for agglutinates to form, and such collisions must occur over time scales substantially shorter than for the entity to actually permeate through the biogel. For instance, HIV virions generally only experience up to one or two collisions over a 12-hour period at concentrations similar to those found in semen of acutely infected males, which possess by far the highest viral titers.[116] This pattern is true of other viruses and non-motile bacteria that are commonly transmitted vaginally: appreciable collisions simply do not occur even at concentrations equal to the maximal titers present in semen from acutely infected individuals. In these instances, it is unlikely that agglutination would be an effective barrier mechanism. Collision frequency increases with greater mobility: at the same concentration, a swimming bacterium is much more likely to encounter another bacterium than a non-motile bacterium that could only undergo Brownian diffusion. However, even with the typical bacterial load in the GI tract, the collisions between bacteria may be relatively limited.[103]

4.2.2 Crosslinkers that facilitate enchained growth

Classical agglutination describes distinct bodies colliding and becoming bound together and requires a high density of pathogen (>10^8 colony forming units [CFU]/gram). However, typical infections occur with far lower concentrations (10^0-

10^7 CFU/g). Moor *et al.*[108] addressed this discrepancy with a mouse model of oral vaccination against *S. typhimurium* to demonstrate enchained growth as a function of sIgA (Figure 9). Specifically, mice were orally vaccinated with an inactivated strain of *S. typhimurium* and challenged with wild type *S. typhimurium* possessing different fluorophores. Bacteria from vaccinated mice were densely coated with specific sIgA and formed large, unicolor clumps, implying each clump originated from an individual bacterial cell. The authors therefore proposed enchained growth as the dominant mechanism of inducing bacterial aggregation vs. agglutination, in which sIgA bound to the mother cell crosslinks daughter cells, resulting in a chain of linked cells. This results in an immobile mass of bacterial cells that cannot permeate through mucus and limits bacterial growth via quorum sensing.

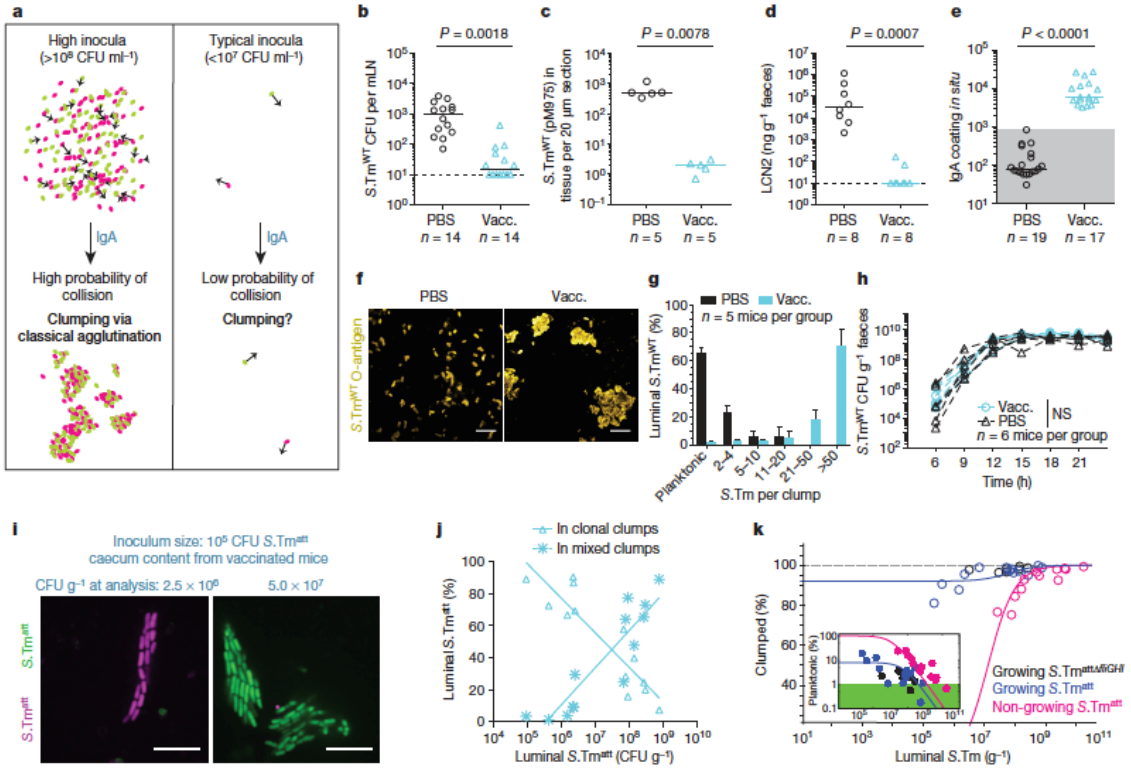

Figure 9. Enchained growth is a protective mechanism in nontyphoidal salmonellosis. a, Density-dependence of agglutination. b–g, Mock- (PBS) or PA-S.Tm-vaccinated (vacc.) mice were pretreated with streptomycin, infected (10^5 CFU, indicated strain, by gavage) and analysed 18 h later. Pathogen loads in mLN (CFU) (b) or epithelium and lamina propria (microscopy) (c). d, Faecal lipocalin-2 (LCN2). e, IgA-coating of wild-type S. Typhimurium ($S.Tm^{WT}$) (caecum content;). f, g, S. Typhimurium clumping in caecum lumen (frozen sections; scale bar, 10 μm; mean ± s.d.). h, Faecal $S.Tm^{WT}$. NS, not significant (repeat-measures ANOVA). i–k, PA-S.Tm-vaccinated mice were challenged with a 1:1-mix of mCherry- and GPF-tagged $S.Tm^{att}$ (10^5 CFU). Images of live caecal content (3–8 h after infection). i, Representative images (5 h after infection). j, Clump clonality plotted against luminal CFU density (n = 13). k, Confocal microscopy quantification of clumping from mice infected with 10^5 CFU $S.Tm^{att}$ (blue circles, n = 13) or $S.Tm^{attΔfliGHI}$ (black circles, n = 7) and 10^{10} CFU $S.Tm^{att}$ or 10^9 PFA-fixed $S.Tm^{att}$ (magenta circles, n = 12). Lines show robust fittings of the enchained growth/agglutination model, green area represents parameter space where less than 1% luminal S.Tm are planktonic. Dashed line, detection limit; grey-shaded areas, background levels. Unless otherwise stated, statistics are the results of two-tailed Mann–Whitney U-tests. Horizontal lines represent median. Figure from [108].

Crosslinks between sIgA and enchained bacteria are not permanent due to natural unbinding rates and shear stresses produced by the mixing required for efficient digestion. Bansept *et al.*[107] modeled the effect of crosslink time and bacterial replication rates on concentration of free bacteria and cluster sizes. They included models accounting for bacterial escape and loss due to excretion, fixed bacterial replication time vs. rate, independent linear chains after breaking of chains, and force-dependent breaking rates. In all models, a general pattern emerged: bacteria growing at slower rates (i.e. commensal, non-pathogenic bacteria) than the rate of linkage breaking existed mostly as free bacteria, while rapidly dividing bacteria (i.e. pathogenic or dysbiotic bacteria) replicating much faster than linkage breaking formed immobile clusters. This implies that crosslinkers that facilitate enchained growth would be most effective against rapidly

dividing bacteria, regardless of the bacterial concentration, but less so against low titers of bacteria that divide slowly.

4.3 Advantages and disadvantages of tuning biogels using third party modulators

The primary advantages of utilizing third-party crosslinkers are their abilities to mediate selective trapping of specific pathogens without broadly perturbing other properties of the biogels. The weak crosslinker-matrix affinity allows for flexibility in addition of crosslinkers, ensuring quick and uniform distribution of the crosslinkers within a biogel, as we had previously observed with topical passive immunization of the vagina with IgG. In the production of any synthetic biogels, crosslinkers can also be incorporated before gelation to ensure even more uniform mixing.

The weak crosslinker-matrix affinity prevents saturation of binding sites on matrix constituents and consequently, greatly increases the ability to simultaneously trap a diverse array of foreign particles. To demonstrate this, we treated Matrigel® with 1:100 ratio of anti-PEG and anti-biotin antibodies. The presence of excess anti-biotin IgG did not interfere with the ability of anti-PEG antibody to trap PEGylated nanoparticles.[38] This underscores the ability to quickly and easily tune the barrier properties of biogels that cannot be accomplished by modifying the biochemistry of a biogel matrix.

Matrix-binding crosslinkers must accumulate on foreign particles in sufficient quantity to mediate trapping. This implies that they could be saturated with high concentrations of foreign particles. One method to overcome the limit is to

utilize third-party, polyvalent agglutinating modulators that can induce formation of aggregates. Agglutination is most effective when particles have a high frequency of collision, either due to a high concentration of from inherent active motility. If the target is replicative, polyvalent antibodies may also induce a non-classical form of aggregation through enchained growth.

The greatest strength with using third-party modulators to modulate the biogel barrier is also its primary disadvantage: the specificities conferred by the crosslinker imply that we are only able to enhance the barrier against a finite number of species that were identified *a priori*. Given the diversity of foreign entities to which a biogel may be exposed, methods that can enable exclusion strictly based on size or charge may turn out to be more practical.

5 Conclusion

Given biogels' multifaceted functions, having diverse methods to modulate their barrier properties (as summarized in Table 4) is essential for realizing the full range of their potential applications. While there is a longstanding history of tuning the pore sizes of a biogel as well as the composition of the biogel matrix to enhance the steric and adhesive barrier properties of biogels, the use of third-party modulators to tune biogel barrier is a recently emerged strategy with the potential to greatly increase the flexibility, ease and throughput. For instance, it is now possible to directly tune the barrier properties of mucus lining exposed tissues in the body against foreign pathogens simply by dosing pathogen-specific antibodies to mucosal surfaces, without the need to otherwise alter the physical and biochemical

properties of mucus that may lead to adverse health consequences. Likewise, such third-party modulators may improve retention of cells within a hydrogel for various tissue engineering and cell therapy applications.[87,117]

	Advantages	Disadvantages
Steric Hindrance	Required component of any barrier strategy Capable of boardly excluding all species based solely on size	Tuning frequently alters gel rheology Excess tuning may overly exclude particles No molecular specificity
Adhesive Interactions	Somewhat specific Can be engineered into *de novo* biogels for improved specificity	Tuning methods may alter physical properties of gel Engineering to incorporate specificity is inherently low-throughput
Third-Party Modulators	Most specific Multiple species can be trapped simultaneously Tuning does not alter biogel structure Can be added to biogel before or after gelation	Requires knowledge of foreign species to be trapped, with modulators that possess specific affinity to those species Agglutinating modulators may have limited potency when foreign species are present at very low concentration Specific matrix affinity required for matrix-binding crosslinkers; may require tuning of matrix-binding domain for biogel compatibility

Table 4. Summary of advantages and disadvantages of methods to tune barrier properties of biological hydrogels.

When developing gels for biomedical applications, there are likely stringent requirements for both their rheological properties as well as chemical composition. Generally, applied biogels should mimic the stiffness and viscosity of surrounding tissues to prevent unwanted cellular response due to aberrant mechanical signaling. Most biogels must also allow for selective permeation of essential nutrients and cells. Such requirements may restrict the ability to tune the nanoscale and

microscale barrier properties of biogels based on steric hindrance and/or direct adhesive interactions alone. The use of third-party modulators avoid these pitfalls, and may provide important flexibility to tune biogels with molecular specificity in these instances.

To tune biogels with third-party modulators, one must have prior knowledge of the foreign species of interest at the molecular level in order to bind the foreign species. The type of modulators also depend on specific applications: agglomerating modulators are inherently more potently at limiting permeation of actively motile, larger species present at high local concentrations, best exemplified by rapidly dividing bacteria or sperm. Matrix-interacting third-party modulators are more effective at limiting transport of smaller species that undergo Brownian diffusion, such as viruses. Depending on the precise application, the challenge may involve sustaining effective concentrations of these modulators within a biogel over time.

Finally, the use of third-party modulators to tune biogels as a field is still in its infancy. This strategy can be coupled with methods to tune the steric obstruction and/or adhesive properties of biogels to further enhance the range of potential applications. Likewise, incorporating stimuli-responsive elements will likely further expand the range of applications.

6 Acknowledgements

This work was supported by the Eshelman Institute for Innovation, National Institutes of Health (http://www.nih.gov/; Grants R01HL141934 and R01HD101562 (S.K.L.); the National Science Foundation DMR-1810168 (S.K.L.); the David and Lucile Packard Foundation (http://www.packard.org/; Grant 2013-39274; S.K.L.); and PhRMA Foundation Predoctoral Fellowship (J.L.S.). The funders had no role in decision to publish or preparation of the manuscript.

7 Conflict of Interest Disclosure

Mucommune, LLC and Inhalon Biopharma, Inc both seek to harness antibody-mucin interactions to improve protection against or treatment of infections at mucosal surfaces, and have licensed intellectual property from the University of North Carolina - Chapel Hill (UNC-CH). SKL is an inventor on issued and pending patents licensed by both companies, is a founder of both Mucommune and Inhalon, and owns company stock. SKL's relationships with Mucommune and with Inhalon are subject to certain restrictions under University policy. The terms of this arrangement are being managed by UNC-CH in accordance with its conflict of interest policies. JLS is an inventor on a pending patent licensed by both Mucommune and Inhalon.

8 References

1 Hoffman AS. Hydrogels for biomedical applications. *Adv Drug Del Rev* **64,** 3-12 (2002).

2 Lee KY & Mooney DJ. Alginate: Properties and biomedical applications. *Prog Polym Sci* **37,** 106-126 (2012).

3 Achilli M & Mantovani D. Tailoring mechanical properties of collagen-based scaffolds for vascular tissue engineering: The effects of pH, temperature and ionic strength on gelation. *Polymers* **2,** 664-680 (2010).

4 Tako M. The principle of polysaccharide gels. *Adv Biosci Biotechnol* **06,** 22-36 (2015).

5 Lin Y, Xia X, Shang K, Elia R, Huang W, Cebe P, Leisk G, Omenetto F, & Kaplan DL. Tuning chemical and physical cross-links in silk electrogels for morphological analysis and mechanical reinforcement. *Biomacromolecules* **14,** 2629-2635 (2013).

6 Ahmadi F, Oveisi Z, Mohammadi Samani S, & Amoozgar Z. Chitosan based hydrogels: Characteristics and pharmaceutical applications. *Res Pharm Sci* **10,** 1-16 (2015).

7 Augst AD, Kong HJ, & Mooney DJ. Alginate hydrogels as biomaterials. *Macromol Biosci* **6,** 623-633 (2006).

8 Jin R, Teixeira LS, Dijkstra PJ, van Blitterswijk CA, Karperien M, & Feijen J. Enzymatically-crosslinked injectable hydrogels based on biomimetic dextran-hyaluronic acid conjugates for cartilage tissue engineering. *Biomaterials* **31,** 3103-3113 (2010).

9 Cone RA. Barrier properties of mucus. *Adv Drug Del Rev* **61,** 75-85 (2009).

10 Cornick S, Tawiah A, & Chadee K. Roles and regulation of the mucus barrier in the gut. *Tissue Barriers* **3,** e982426 (2015).

11 Duncan GA, Jung J, Hanes J, & Suk JS. The mucus barrier to inhaled gene therapy. *Mol Ther* **24,** 2043-2053 (2016).

12 Wagner CE, Wheeler KM, & Ribbeck K. Mucins and their role in shaping the function of mucus barriers. *Annu Rev Cell Dev Biol* **34,** 189-215 (2018).

13 Billings N, Birjiniuk A, Samad TS, Doyle PS, & Ribbeck K. Material properties of biofilms-a review of methods for understanding permeability and mechanics. *Rep Prog Phys* **78,** 036601 (2015).

14 Dufour D, Leung V, & Lévesque CM. Bacterial biofilm: Structure, function, and antimicrobial resistance. *Endontic Topics* **22,** 2-16 (2012).

15 Flemming H-C & Wingender J. The biofilm matrix. *Nat Rev Microbiol* **8,** 623-633 (2010).

16 Steukers L, Glorieux S, Vandekerckhove AP, Favoreel HW, & Nauwynck HJ. Diverse microbial interactions with the basement membrane barrier. *Trends Microbiol* **20,** 147-155 (2012).

17 Schuster BS, Suk JS, Woodworth GF, & Hanes J. Nanoparticle diffusion in respiratory mucus from humans without lung disease. *Biomaterials* **34,** 3439-3446 (2013).

18 Murgia X, Pawelzyk P, Schaefer UF, Wagner C, Willenbacher N, & Lehr C-M. Size-limited penetration of nanoparticles into porcine respiratory mucus after aerosol deposition. *Biomacromolecules* **17,** 1536-1542 (2016).
19 Lai SK, O'Hanlon DE, Harrold S, Man ST, Wang Y-Y, Cone R, & Hanes J. Rapid transport of large polymeric nanoparticles in fresh undiluted human mucus. *Proc Natl Acad Sci USA* **104,** 1482-1487 (2007).
20 Lai SK, Wang Y-Y, Hida K, Cone R, & Hanes J. Nanoparticles reveal that human cervicovaginal mucus is riddled with pores larger than viruses. *Proc Natl Acad Sci USA* **107,** 598-603 (2010).
21 Nance EA, Woodworth GF, Sailor KA, Shih T-Y, Xu Q, Swaminathan G, Xiang D, Eberhart CG, & Hanes J. A dense poly(ethylene glycol) coating improves penetration of large polymeric nanoparticles within brain tissue. *Sci Transl Med* **4,** 149ra119 (2012).
22 Albanese A, Lam AK, Sykes EA, Rocheleau JV, & Chan WC. Tumour-on-a-chip provides an optical window into nanoparticle tissue transport. *Nat Commun* **4,** 2718 (2013).
23 Dancy JG, Wadajkar AS, Schneider CS, Mauban JRH, Woodworth GF, Winkles JA, & Kim AJ. Non-specific binding and steric hindrance thresholds for penetration of particulate drug carriers within tumor tissue. *J Control Release* **238,** 139-148 (2016).
24 Erikson A, Andersen HN, Naess SN, Sikorski P, & de Lange Davies C. Physical and chemical modifications of collagen gels: Impact on diffusion. *Biopolymers* **89,** 135-143 (2008).
25 Scherer P, Kluge M, Klein J, & Sahm H. Immobilization of the methanogenic bacterium *Methanosarcina barkeri*. *Biotechnol Bioeng* **23,** 1057-1065 (1981).
26 Klein J, Stock J, & Vorlop K-D. Pore size and properties of spherical Ca-alginate biocatalysts. *Eur J Appl Microbiol Biotechnol* **18,** 86-91 (1983).
27 Ramanujuan S, Pluen A, McKee TD, Brown EB, Boucher Y, & Jain RK. Diffusion and convection in collagen gels: Implications for transport in the tumor interstitium. *Biophys J* **83,** 1650-1660 (2002).
28 Yang R, Tan L, Cen L, & Zhang Z. An injectable scaffold based on crosslinked hyaluronic acid gel for tissue regeneration. *RSC Adv* **6,** 16838-16850 (2016).
29 Lin H, Liu J, Zhang K, Fan Y, & Zhang X. Dynamic mechanical and swelling properties of maleated hyaluronic acid hydrogels. *Carbohydr Polym* **123,** 381-389 (2015).
30 Lorén N, Shtykova L, Kidman S, Jarvoll P, Nydén M, & Hermansson A-M. Dendrimer diffusion in κ-carrageenan gel structures. *Biomacromolecules* **10,** 275-284 (2009).
31 de Kort DW, van Duynhoven JPM, Hoeben FJM, Janssen HM, & Van As H. NMR nanoparticle diffusometry in hydrogels: Enhancing sensitivity and selectivity. *Anal Chem* **86,** 9229-9235 (2014).
32 Pluen A, Netti PA, Jain RK, & Berk DA. Diffusion of macromolecules in agarose gels: Comparison of linear and globular configurations. *Biophys J* **77,** 542-552 (1999).

33 Krajewska B & Olech A. Pore structure of gel chitosan membranes. I. Solute diffusion measurements. *Polym Gels Networks* **4,** 33-43 (1996).
34 Falk B, Garramone S, & Shivkumar S. Diffusion coefficient of paracetamol in a chitosan hydrogel. *Mater Lett* **58,** 3261-3265 (2004).
35 Arends F, Baumgärtel RM, & Lieleg O. Ion-specific effects modulate the diffusive mobility of colloids in an extracellular matrix gel. *Langmuir* **29,** 15965-15973 (2013).
36 Arends F, Nowald C, Pflieger K, Boettcher K, Zahler S, & Lieleg O. The biophysical properties of basal lamina gels depend on the biochemical composition of the gel. *PLoS One* **10,** e0118090 (2015).
37 Arends F, Sellner S, Seifert P, Gerland U, Rehberg M, & Lieleg O. A microfluidics approach to study the accumulation of molecules at basal lamina interfaces. *Lab Chip* **15,** 3326-3334 (2015).
38 Schiller JL, Marvin A, McCallen JD, & Lai SK. Robust antigen-specific tuning of the nanoscale barrier properties of biogels using matrix-associating IgG and IgM antibodies. *Acta Biomater* **89,** 95-103 (2019).
39 Henry CE, Wang Y-Y, Yang Q, Hoang T, Chattopadhyay S, Hoen T, Ensign LM, Nunn KL, Schroeder H, McCallen J, Moench T, Cone R, Roffler SR, & Lai SK. Anti-PEG antibodies alter the mobility and biodistribution of densely PEGylated nanoparticles in mucus. *Acta Biomater* **43,** 61-70 (2016).
40 Käsdorf BT, Arends F, & Lieleg O. Diffusion regulation in the vitreous humor. *Biophys J* **109,** 2171-2181 (2015).
41 Xu Q, Boylan NJ, Suk JS, Wang Y-Y, Nance EA, Yang J-C, McDonnell PJ, Cone RA, Duh EJ, & Hanes J. Nanoparticle diffusion in, and microrheology of, the bovine vitreous *ex vivo*. *J Control Release* **167,** 76-84 (2013).
42 Lieleg O, Vladescu I, & Ribbeck K. Characterization of particle translocation through mucin hydrogels. *Biophys J* **98,** 1782-1789 (2010).
43 Cu Y & Saltzman WM. Controlled surface modification with poly(ethylene)glycol enhances diffusion of PLGA nanoparticles in human cervical mucus. *Mol Pharm* **6,** 173-181 (2009).
44 Wang Y-Y, Kannan A, Nunn KL, Murphy MA, Subramani DB, Moench TR, Cone RA, & Lai SK. IgG in cervicovaginal mucus traps HSV and prevents vaginal herpes infections. *Mucosal Immunol* **7,** 1036-1044 (2014).
45 Wang Y-Y, Nunn KL, Harit D, McKinley SA, & Lai SK. Minimizing biases associated with tracking analysis of submicron particles in heterogeneous biological fluids. *J Control Release* **220,** 37-43 (2015).
46 Valentine MT, Perlman ZE, Gardel ML, Shin JH, Matsudaira P, Mitchison TJ, & Weitz DA. Colloid surface chemistry critically affects multiple particle tracking measurements of biomaterials. *Biophys J* **86,** 4004-4014 (2004).
47 Schiller JL, Fogle MM, Bussey O, Kissner WJ, Hill DB, & Lai SK. Antibody-mediated trapping in biological hydrogels is governed by sugar-sugar hydrogen bonds. *Acta Biomater* **107,** 91-101 (2020).
48 Yang B, Schaefer A, Wang Y-Y, McCallen JD, Lee P, Newby JM, Arora H, Kumar PA, Zeitlin L, Whaley KJ, McKinley SA, Fischer WA, 2nd, Harit D, & Lai SK.

ZMapp reinforces the airway mucosal barrier against Ebola virus. *J Infect Dis* **218,** 901-910 (2018).

49 Suk JS, Kim AJ, Trehan K, Schneider CS, Cebotaru L, Woodward OM, Boylan NJ, Boyle MP, Lai SK, Guggino WB, & Hanes J. Lung gene therapy with highly compacted DNA nanoparticles that overcome the mucus barrier. *J Control Release* **178,** 8-17 (2014).

50 Nunn KL, Wang Y-Y, Harit D, Humphrys MS, Ma B, Cone R, Ravel J, & Lai SK. Enhanced trapping of HIV-1 by human cervicovaginal mucus is associated with *Lactobacillus crispatus*-dominant microbiota. *MBio* **6,** e01084-01015 (2015).

51 Olmsted SS, Padgett JL, Yudin AI, Whaley KJ, Moench TR, & Cone RA. Diffusion of macromolecules and virus-like particles in human cervical mucus. *Biophys J* **81,** 1930-1937 (2001).

52 Abdulkarim M, Agulló N, Cattoz B, Griffiths PC, Bernkop-Schnürch A, Borros SG, & Gumbleton M. Nanoparticle diffusion within intestinal mucus: Three-dimensional response analysis dissecting the impact of particle surface charge, size and heterogeneity across polyelectrolyte, pegylated and viral particles. *Eur J Pharm Biopharm* **97,** 230-238 (2015).

53 Hansing J, Duke JR, 3rd, Fryman EB, DeRouchey JE, & Netz RR. Particle diffusion in polymeric hydrogels with mixed attractive and repulsive interactions. *Nano Lett* **18,** 5248-5256 (2018).

54 Griffiths PC, Cattoz B, Ibrahim MS, & Anuonye JC. Probing the interaction of nanoparticles with mucin for drug delivery applications using dynamic light scattering. *Eur J Pharm Biopharm* **97,** 218-222 (2015).

55 Stylianopoulos T, Poh M-Z, Insin N, Bawendi MG, Fukumura D, Munn LL, & Jain RK. Diffusion of particles in the extracellular matrix: The effect of repulsive electrostatic interactions. *Biophys J* **99,** 1342-1349 (2010).

56 Ensign LM, Henning A, Schneider CS, Maisel K, Wang Y-Y, Porosoff MD, Cone RA, & Hanes J. *Ex vivo* characterization of particle transport in mucus secretions coating freshly excised mucosal tissues. *Mol Pharm* **10,** 2176-2182 (2013).

57 Ensign LM, Tang BC, Wang Y-Y, Tse TA, Hoen T, Cone RA, & Hanes J. Mucus-penetrating nanoparticles for vaginal drug delivery protect against herpes simplex virus. *Sci Transl Med* **4,** 138ra179 (2012).

58 Gilli P, Pretto L, Bertolasi V, & Gilli G. Predicting hydrogen-bond strengths from acid-base molecular properties. The pK(a) slide rule: toward the solution of a long-lasting problem. *Acc Chem Res* **42,** 33-44 (2009).

59 Larhed AW, Artursson P, & Björk E. The influence of intestinal mucus components on the diffusion of drugs. *Pharm Res* **15,** 66-71 (1998).

60 Larhed AW, Artursson P, Gråsjö J, & Björk E. Diffusion of drugs in native and purified gastrointestinal mucus. *J Pharm Sci* **86,** 660-665 (1997).

61 Groo A-C, Saulnier P, Gimel JC, Gravier J, Ailhas C, Benoit J-P, & Lagarce F. Fate of paclitaxel lipid nanocapsules in intestinal mucus in view of their oral delivery. *Int J Nanomed* **8,** 4291-4302 (2013).

62 Lai SK, Hida K, Shukair S, Wang Y-Y, Figueiredo A, Cone R, Hope TJ, & Hanes J. Human immunodeficiency virus type 1 is trapped by acidic but not by neutralized human cervicovaginal mucus. *J Virol* **83,** 11196-11200 (2009).
63 Kloxin AM, Kasko AM, Salinas CN, & Anseth KS. Photodegradable hydrogels for dynamic tuning of physical and chemical properties. *Science* **324,** 59-63 (2009).
64 Suk JS, Lai SK, Boylan NJ, Dawson MR, Boyle MP, & Hanes J. Rapid transport of muco-inert nanoparticles in cystic fibrosis sputum treated with N-acetyl cysteine. *Nanomedicine (Lond)* **6,** 365-375 (2011).
65 Schultz KM & Anseth KS. Monitoring degradation of matrix metalloproteinases-cleavable PEG hydrogels via multiple particle tracking microrheology. *Soft Matter* **9,** 1570-1579 (2013).
66 Collins MN & Birkinshaw C. Morphology of crosslinked hyaluronic acid porous hydrogels. *J Appl Polym Sci* **120,** 1040-1049 (2011).
67 Sacco P, Paoletti S, Cok M, Asaro F, Abrami M, Grassi M, & Donati I. Insight into the ionotropic gelation of chitosan using tripolyphosphate and pyrophosphate as cross-linkers. *Int J Biol Macromol* **92,** 476-483 (2016).
68 Ullah F, Othman MBH, Javed F, Ahmad Z, & Akil HM. Classification, processing and application of hydrogels: A review. *Materials Science and Engineering C* **57,** 414-433 (2015).
69 Akhtar MF, Hanif M, & Ranjha NM. Methods of synthesis of hydrogels … A review. *Saudi Pharmaceutical Journal* **24,** 554-559 (2016).
70 Annabi N, Nichol JW, Zhong X, Ji C, Koshy ST, Khademhosseini A, & Denghani F. Controlling the porosity and microarchitecture of hydrogels for tissue engineering. *Tissue Eng Part B* **16,** 371-383 (2010).
71 Sell SA, Wolfe PS, Garg K, McCool JM, Rodriguez I, A., & Bowlin GL. The use of natural polymers in tissue engineering: A focus on electrospun extracellular matrix analogues. *Polymers* **2,** 522-553 (2010).
72 Kim U-J, Park J, Kim HJ, Wada M, & Kaplan DL. Three-dimensional aqueous-derived biomaterial scaffolds from silk fibroin. *Biomaterials* **26,** 2775-2785 (2005).
73 Mandal BB & Kundu SC. Cell proliferation and migration in silk fibroin 3D scaffolds. *Biomaterials* **30,** 2956-2965 (2009).
74 Huang L, Huang J, Shao H, Hu X, Cao C, Fan S, Song L, & Zhang Y. Silk scaffolds with gradient pore structure and improved cell infiltration performance. *Mater Sci Eng C Mater Biol Appl* **94,** 179-189 (2019).
75 Vedadghavami A, Minooei F, Mohammadi MH, Khetani S, Rezaei Kolahchi A, Mashayekhan S, & Sanati-Nezhad A. Manufacturing of hydrogel biomaterials with controlled mechanical properties for tissue engineering applications. *Acta Biomater* **62,** 42-63 (2017).
76 Bajaj P, Schweller RM, Khademhosseini A, West JL, & Bashir R. 3D biofabrication strategies for tissue engineering and regenerative medicine. *Annu Rev Biomed Eng* **16,** 247-276 (2014).

77 Apgar J, Tseng Y, Federov E, Herwig MB, Almo SC, & Wirtz D. Multiple-particle tracking measurements of heterogeneities in solutions of actin filaments and actin bundles. *Biophys J* **79,** 1095-1106 (2000).
78 Magzoub M, Jin S, & Verkman AS. Enhanced macromolecule diffusion deep in tumors after enzymatic digestion of extracellular matrix collagen and its associated proteoglycan decorin. *FASEB J* **22,** 276-284 (2008).
79 Li X, Fu M, Wu J, Zhang C, Deng X, Dhinakar A, Huang W, Qian H, & Ge L. pH-sensitive peptide hydrogel for glucose-responsive insulin delivery. *Acta Biomater* **51,** 294-303 (2017).
80 Webber MJ & Anderson DG. Smart approaches to glucose-responsive drug delivery. *J Drug Targeting* **23,** 651-655 (2015).
81 VandenBerg MA & Webber MJ. Biologically inspired and chemically derived methods for glucose-responsive insulin therapy. *Adv Healthc Mater* **8,** e1801466 (2019).
82 Acar H, Srivastava S, Chung EJ, Schnorenberg MR, Barrett JC, LaBelle JL, & Tirrell M. Self-assembling peptide-based building blocks in medical applications. *Adv Drug Del Rev* **110-111,** 65-79 (2017).
83 Chen J & Zou X. Self-assemble peptide biomaterials and their biomedical applications. *Bioact Mater* **4,** 120-131 (2019).
84 Liu R & Hudalla GA. Using self-assembling peptides to integrate biomolecules into functional supramolecular biomaterials. *Molecules* **24,** 1450 (2019).
85 Gelain F, Unsworth LD, & Zhang S. Slow and sustained release of active cytokines from self-assembling peptide scaffolds. *J Control Release* **145,** 231-239 (2010).
86 Freudenberg U, Atallah P, Limasale YDP, & Werner C. Charge-tuning of glycosaminoglycan-based hydrogels to program cytokine sequestration. *Faraday Discuss* (2019).
87 Bodenberger N, Kubiczek D, Halbgebauer D, Rimola V, Wiese S, Mayer D, Rodriguez Alfonso AA, Ständker L, Stenger S, & Rosenau F. Lectin-functionalized composite hydrogels for "capture-and-killing" of carbapenem-resistant *Pseudomonas aeruginosa*. *Biomacromolecules* **19,** 2472-2482 (2018).
88 Koshi Y, Nakata E, Yamane H, & Hamachi I. A fluorescent lectin array using supramolecular hydrogel for simple detection and pattern profiling for various glycoconjugates. *J Am Chem Soc* **128,** 10413-10322 (2006).
89 Mabry KM, Schroeder ME, Payne SZ, & Anseth KS. Three-dimensional high-throughput cell encapsulation platform to study changes in cell-matrix interactions. *ACS Appl Mater Interfaces* **8,** 21914-21922 (2016).
90 Sun Y, Li W, Wu X, Zhang N, Zhang Y, Ouyang S, Song X, Fang X, Seeram R, Xue W, He L, & Wu W. Functional self-assembling peptide nanofiber hydrogels designed for nerve degeneration. *ACS Appl Mater Interfaces* **8,** 2348-2359 (2016).

91 Jiang B, Yang J, Rahoui N, Taloub N, & Huang YD. Functional polymer materials affecting cell attachment. *Adv Colloid Interface Sci* **250,** 185-194 (2017).
92 Turturro MV, Sokic S, Larson JC, & Papavasiliou G. Effective tuning of ligand incorporation and mechanical properties in visible light photopolymerized poly(ethylene glycol) diacrylate hydrogels dictates cell adhesion and proliferation. *Biomed Mater* **8,** 025001 (2013).
93 Shu XZ, Ghosh K, Liu Y, Palumbo FS, Luo Y, Clark RA, & Prestwich GD. Attachment and spreading of fibroblasts on an RGD peptide–modified injectable hyaluronan hydrogel. *J Biomed Mater Res A* **68,** 365-375 (2004).
94 Saltzman WM, Radomsky ML, Whaley KJ, & Cone RA. Antibody diffusion in human cervical mucus. *Biophys J* **66,** 506-515 (1994).
95 Zhang R, Tang M, Bowyer A, Eisenthal R, & Hubble J. A novel pH- and ionic-strength-sensitive carboxy methyl dextran hydrogel. *Biomaterials* **26,** 4677-4683 (2005).
96 Rosales AM & Anseth KS. The design of reversible hydrogels to capture extracellular matrix dynamics. *Nat Rev Mater* **1** (2016).
97 Segura T, Anderson BC, Chung PH, Webber RE, Shull KR, & Shea LD. Crosslinked hyaluronic acid hydrogels: A strategy to functionalize and pattern. *Biomaterials* **26,** 359-371 (2005).
98 Branco de Cunha C, Klumpers DD, Li WA, Koshy ST, Weaver JC, Chaudhuri O, Granja PL, & Mooney DJ. Influence of the stiffness of three-dimensional alginate/collagen-I interpenetrating networks on fibroblast biology. *Biomaterials* **35,** 8927-8936 (2014).
99 Newby J, Schiller JL, Wessler T, Edelstein J, Forest MG, & Lai SK. A blueprint for robust crosslinking of mobile species in biogels with weakly adhesive molecular anchors. *Nat Commun* **8,** 833 (2017).
100 Wessler T, Chen A, McKinley SA, Cone R, Forest MG, & Lai SK. Using computational modeling to optimize the design of antibodies that trap viruses in mucus. *ACS Infect Dis* **2,** 82-92 (2016).
101 Chen A, McKinley SA, Wang S, Shi F, Mucha PJ, Forest MG, & Lai SK. Transient antibody-mucin interactions produce a dynamic molecular shield against viral invasion. *Biophys J* **106,** 2028-2036 (2014).
102 Schroeder HA, Newby J, Schaefer A, Subramani B, Tubbs A, Forest MG, Miao E, & Lai SK. LPS-binding IgG arrests actively motile *Salmonella Typhimurium* in gastrointestinal mucus. *Mucosal Immunol***,** in press (2020).
103 Xu F, Newby JM, Schiller JL, Schroeder HA, Wessler T, Chen A, Forest MG, & Lai SK. Modeling barrier properties of intestinal mucus reinforced with IgG and secretory IgA against motile bacteria. *ACS Infect Dis* (2019).
104 Jager S, Kremer J, Kuiken J, & Mulder I. The significance of the Fc part of antispermatozoal antibodies for the shaking phenomenon in the sperm-cervical mucus contact test. *Fertil Steril* **36,** 792-797 (1981).
105 Kremer J & Jager S. Sperm-cervical mucus interaction, in particular in the presence of antispermatozoal antibodies. *Hum Reprod* **3,** 69-73 (1988).

106 Kremer J & Jager S. The significance of antisperm antibodies for sperm--cervical mucus interaction. *Hum Reprod* **7,** 781-784 (1992).
107 Bansept F, Schumann-Moor K, Diard Mdr, Hardt W-D, Slack E, & Loverdo C. Enchained growth and cluster dislocation: A possible mechanism for microbiota homeostasis. *PLoS Comp Biol* **15,** e1006986 (2019).
108 Moor K, Diard M, Sellin ME, Felmy B, Wotzka SY, Toska A, Bakkeren E, Arnoldini M, Bansept F, Dal Co A, Völler T, Minola A, Fernandez-Rodriguez B, Agatic G, Barbieri S, Piccoli L, Casiraghi C, Corti D, Lanzavecchia A, Regoes RR, Loverdo C, Stocker R, Brumley DR, Hardt W-D, & Slack E. High-avidity IgA protects the intestine by enchaining growing bacteria. *Nature* **544,** 498-502 (2017).
109 Schroeder HA, Nunn KL, Schaefer A, Henry CE, Lam F, Pauly MH, Whaley KJ, Zeitlin L, Humphrys MS, Ravel J, & Lai SK. Herpes simplex virus-binding IgG traps HSV in human cervicovaginal mucus across the menstrual cycle and diverse vaginal microbial composition. *Mucosal Immunol* **11,** 1477-1486 (2018).
110 Wang Y-Y, Harit D, Subramani DB, Arora H, Kumar PA, & Lai SK. Influenza-binding antibodies immobilise influenza viruses in fresh human airway mucus. *Eur Respir J* **49,** 1601709 (2017).
111 Arnold JN, Wormald MR, Suter DM, Radcliffe CM, Harvey DJ, Dwek RA, Rudd PM, & Sim RB. Human serum IgM glycosylation: Identification of glycoforms that can bind to mannan-binding lectin. *J Biol Chem* **280,** 29080-29087 (2005).
112 Gilli P & Gilli G. Hydrogen bond models and theories: The dual hydrogen bond model and its consequences. *J Mol Struct* **972,** 2-10 (2010).
113 Mantis NJ, Rol N, & Corthésy B. Secretory IgA's complex roles in immunity and mucosal homeostasis in the gut. *Mucosal Immunol* **4,** 603-611 (2011).
114 Kremer J & Jager S. The sperm-cervical mucus contact test: A preliminary report. *Fertil Steril* **27,** 335-340 (1976).
115 Castle PE, Whaley KJ, Hoen TE, Moench TR, & Cone RA. Contraceptive effect of sperm-agglutinating monoclonal antibodies in rabbits. *Biol Reprod* **56,** 153-159 (1997).
116 Chen A, McKinley SA, Shi F, Wang S, Mucha PJ, Harit D, Forest MG, & Lai SK. Modeling of virion collisions in cervicovaginal mucus reveals limits on agglutination as the protective mechanism of secretory immunoglobulin A. *PLoS One* **10,** e0131351 (2015).
117 Bodenberger N, Kubiczek D, Trösch L, Gawanbacht A, Wilhelm S, Tielker D, & Rosenau F. Lectin-mediated reversible immobilization of human cells into a glycosylated macroporous protein hydrogel as a cell culture matrix. *Sci Rep* **7,** 6151 (2017).